ACS SyntheticBiology

pubs.acs.org/synthbio Letter

High-Titer Production of Olivetolic Acid and Analogs in Engineered Fungal Host Using a Nonplant Biosynthetic Pathway

Ikechukwu C. Okorafor,[‖] Mengbin Chen,[‖] and Yi Tang*

Cite This: *ACS Synth. Biol.* 2021, 10, 2159–2166 Read Online

ACCESS | Metrics & More | Article Recommendations | Supporting Information

ABSTRACT: The microbial synthesis of cannabinoids and related molecules requires access to the intermediate olivetolic acid (OA). Whereas plant enzymes have been explored for *E. coli* and yeast biosynthesis, moderate yields and shunt product formation are major hurdles. Here, based on the chemical logic to form 2,4-dihydroxybenzoate-containing natural products, we discovered a set of fungal tandem polyketide synthases that can produce OA and the related octanoyl-primed derivative sphaerophorolcarboxylic acid in high titers using the model organism *Aspergillus nidulans*. This new set of enzymes will enable new synthetic biology strategies to access microbial cannabinoids.

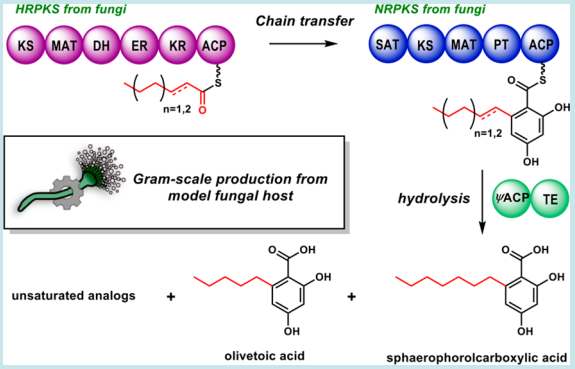

KEYWORDS: *olivetolic acid, fungal pathway, cannabinoids, resorcylic acid, polyketide synthase, genome mining*

INTRODUCTION

Cannabinoids are a large class of bioactive natural products originally derived from the *Cannabis sativa* plant that regulate the cannabinoid receptors CB1 and CB2 of the human endocannabinoid system.[1] Whereas the most well-known cannabinoids are Δ^9-tetrahydrocannabinol (Δ^9-THC) and cannabidiol (CBD), intermediates of the plant cannabinoid biosynthetic pathway, such as tetrahydrocannabinolic acid (THCA), cannabidiolic acid (CBDA), and cannabigerolic acid (CBGA), are also bioactive and useful as ingredients in cannabinoid-based medicines (CBMs) (Figure 1).[2−4] In recent years, there has been significant interest from the synthetic biology community to produce these cannabinoids using microbial and cell-free strategies because of (i) the challenges associated with chemical synthesis, (ii) the inconsistent and relatively low production of cannabinoids from plants, and (iii) the flexibilities in engineering the pathway to access rare or unnatural cannabinoids.[5]

To date, these approaches all rely on the plant pathway, as shown in Figure 1A. The pathway starts with the biosynthesis of the first intermediate olivetolic acid (OA) using two plant enzymes, olivetolic acid synthase (OAS) and olivetolic acid cyclase (OAC). OAS elongates the hexanoyl starter unit from hexanoyl-CoA with malonyl-CoA to yield a tetraketide intermediate. In the absence of OAC, shunt products such as the pyrone and decarboxylated olivetol can form. OAC performs a regioselective aldol cyclization and product release to form OA.[6] OA is then geranylated to form CBGA and is further cyclized by dedicated enzymes to the more advanced cannabinoids. Using the OAS and OAC pair, both *E. coli* and *S. cerevisiae* have been engineered to produce OA and advanced cannabinoids.[7,8] Gonzalez and coworkers demonstrated that ∼80 mg/L of OA can be produced from an *E. coli* strain that accumulates high levels of hexanoyl-CoA, whereas Keasling and coworkers demonstrated the complete reconstitution of THCA and CBDA in yeast starting with OAS and OAC.[7,8] Despite these advances, the use of OAS and OAC in microbial systems suffers from a relatively lower yield of OA (in yeast) and shunt product (pyrone and olivetol) accumulation. Furthermore, new entries into the field are limited by the intellectual property restrictions associated with OAS and OAC. Therefore, alternative pathways that can afford OA and analogs in microbial hosts are highly desired.

OA is a 6-alkyl-substituted 2,4-dihydroxybenzoic acid, also known as a *β*-resorcylic acid.[9,10] The *β*-resorcylate moiety appears frequently in fungal polyketides, including the well-known zearalenone, hypothemycin, and radicicol (Figure 1B).[11,12] In these molecules, the carboxylate group is esterified to form a fused macrolactone, and the resulting molecules are known as resorcylic acid lactones (RALs). The biosynthesis of RALs from fungi has been extensively studied, including contributions from our group.[11,13−17] Two iterative fungal

Received: July 5, 2021
Published: August 20, 2021

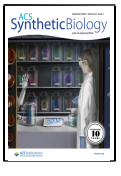

https://doi.org/10.1021/acssynbio.1c00309
ACS Synth. Biol. 2021, 10, 2159−2166

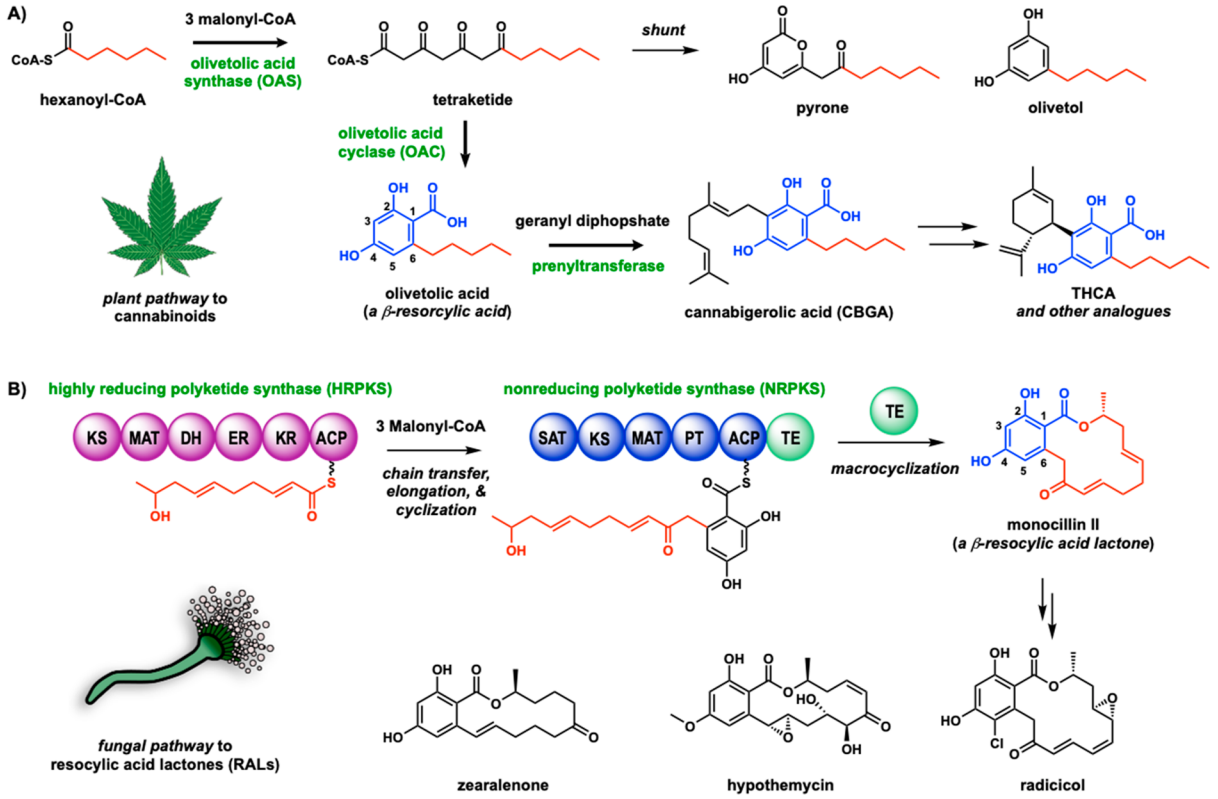

Figure 1. Resorcylic acid natural products produced from *Cannabis sativa* and from fungi. (A) *C. sativa* cannabinoid biosynthetic pathway. The *β*-resorcylic acid, olivetolic acid (OA), is produced from the olivetolic acid synthase (OAS) and olivetolic acid cyclase (OAC). OA is processed to the final products THCA and analogues. In the absence of OAC, side products (pyrone and olivetol) emerge. (B) Tandem fungal iterative polyketide synthases produce resorcylic acid lactones.

polyketide synthases (PKSs) are required to forge the RAL scaffold: A highly reducing PKS (HRPKS) generates the reduced polyketide unit containing the terminal hydroxyl group that becomes the macrocyclizing nucleophile. The chain is transferred to a nonreducing PKS (NRPKS) and further elongated and undergoes aldol cyclization to form the enzyme-bound resorcylic thioester. A fused thioesterase (TE) domain in the NRPKS then performs macrocyclization to release the RAL (e.g., monocillin II in Figure 1B).[16,17] Considerable structural diversity at the C6 position in the RAL can be generated by using different HRPKSs that can synthesize various reduced products.[11]

On the basis of the shared *β*-resorcylate moiety found in OA and in fungal RALs, we hypothesize that fungal biosynthetic pathways that encode a pair of HRPKS and NRPKS may be able to produce OA or related molecules that vary in C6 substitutions. Given the potential to mix-and-match different HRPKS and NRPKS enzymes, such dual-PKS pathways may be engineered to produce different OA derivatives, including those that can lead to rare or unnatural cannabinoids. In this work, we performed genome mining of fungal PKS biosynthetic clusters and identified a set of HRPKS/NRPKS-containing pathways that also encode an unprecedented *ψ*ACP (pseudoacyl carrier protein)-TE enzyme that can release *β*-resorcylic acids such as OA and sphaerophorolcarboxylic acid (SA). The heterologous expression of the pathway in *A. nidulans* led to a high-titer production of OA and SA.

RESULTS AND DISCUSSION

Identification of Potential OA-Producing Pathways in Fungi. The terminal TE domains in the NRPKSs that produce RALs are responsible for the macrocyclization reaction. To produce resorcylic acid instead of RALs, the releasing enzyme must catalyze a hydrolysis reaction instead of esterification. In fungal PKSs, TEs that catalyze hydrolytic release have been characterized and are typically free-standing enzymes.[18] With this in mind, we performed genome mining of sequenced fungal genomes for biosynthetic gene clusters that encode an HRPKS, an NRPKS, and a standalone TE. Among the clusters identified by antiSMASH,[19] one set of homologous clusters satisfied this particular criterion (Figure 2A).

The *ova* cluster from *Metarhizium anisopliae* encodes a typical HRPKS (Ma_OvaA) and an NRPKS (Ma_OvaB) that is not fused to a terminal TE domain. Instead, a didomain enzyme Ma_OvaC containing an N-terminal ACP and a C-terminal TE is present in the cluster. Further sequence analysis of the ACP domain showed that the well-conserved DSL triad in all functional ACPs, in which the serine is post-translationally phosphopantetheinylated, is mutated to NQI.[20−22] This suggests the ACP domain is unlikely to carry out the canonical function of acyl chain shuttling, and thus the enzyme is designated as a *ψ*ACP-TE. Previously, a *ψ*ACP-methyltransferase (MT) fusion enzyme was found in a fungal PKS pathway, in which the *ψ*ACP facilitates protein−protein interactions between the NRPKS and the *ψ*ACP-MT to enable methylation of the growing polyketide intermediate.[23] Hence we hypothesize that the *ψ*ACP domain in Ma_OvaC may have a similar role in facilitating the catalytic function of the TE

https://doi.org/10.1021/acssynbio.1c00309
ACS Synth. Biol. 2021, 10, 2159−2166

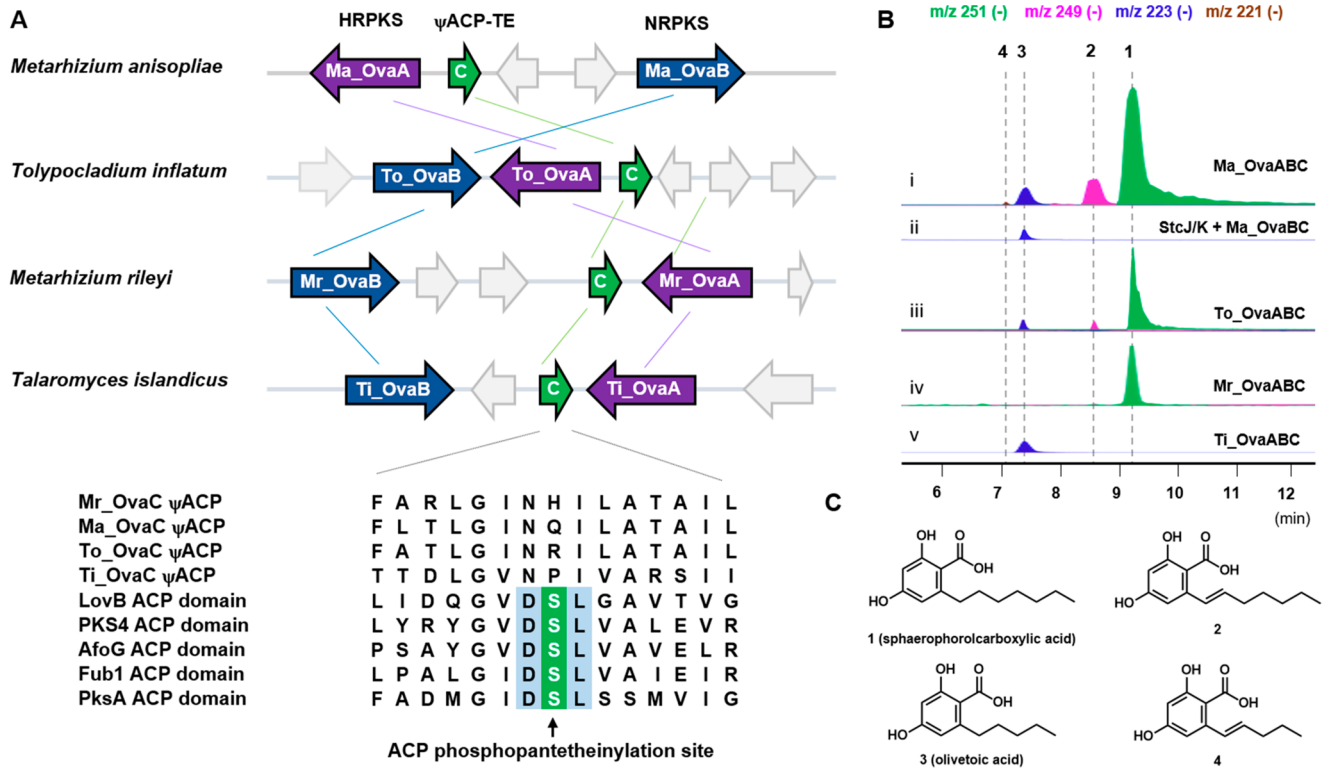

Figure 2. Genome mining of microbial clusters that can synthesize olivetolic acid and related compounds. (A) Homologous clusters were elucidated through genome mining of the ψACP-TE gene. All of the homologous clusters found contained an HRPKS, an NRPKS, and a ψACP-TE. Functional ACPs contain the hallmark DSL sequence, where the serine is post-translationally modified with phosphopantetheine (pPant) and is therefore activated to shuttle the acyl chain. Because the ψACP sequences do not have that serine residue, they cannot be post-translationally modified with pPant and are therefore proposed to be inactive. (B) LC-MS traces of *Aspergillus nidulans* expressing different biosynthetic clusters and combinations of genes. (i) Heterologous expression of Ma_OvaABC from *M. anisopliae* produced compounds **1**−**4**. (ii) Combinatorial biosynthesis of OvaBC with StcJ and StcK fatty acid synthase from *A. nidulans* selectively produced OA. (iii) Heterologous expression of To_OvaABC from *T. inflatum* produced compounds **1**−**3**. (iv) Heterologous expression of Mr_OvaABC from *M. rileyi* primarily produced compound **1**. (v) Heterologous expression of Ti_OvaABC from *T. islandicus* selectively produced compound **3**. (C) Structures of compounds **1**−**4**.

Table 1. Summary of Titers of Olivetolic Acid and Analogues from Heterologous Expression in *A. nidulans*

	1 (mg/L)[a]	**2** (mg/L)	**3** (mg/L)	**4** (mg/L)
Ma_OvaA-C	1400 (±80)	140 (±20)	80 (±10)	0.3
StcJ/K + Ma_OvaB-C	0	0	5 (±1)	0
To_OvaA-C	750 (±20)	75 (±10)	40 (±10)	2 (±1)
Mr_OvaA-C	600 (±10)	60 (±10)	30 (±5)	0.5 (±1)
Ti_OvaA-C	0	0	60 (±10)	0
Ma_OvaA + Ti_OvaB-C	75	0	4	0
Ti_OvaA + Ma_OvaB-C	0	0	0	0

[a]Measurement of titers was performed after 5 days of culturing in 25 mL of CD-ST medium in a 125 mL flask at 28 °C and 250 rpm.

domain on a PKS-bound intermediate. The *M. anisopliae* cluster contains additional genes encoding a transcriptional factor and a flavin-dependent monooxygenase. The alignment of homologous clusters from various fungal species (*Metarhizium rileyi*, *Talaromyces islandicus*, and *Tolypocladium inflatum*) showed that HRPKS, NRPKS, and ψACP-TE are conserved (Figure S1), including the inactivated ACP triad (Figure 2A). None of these clusters has been characterized, and no product has been reported in the literature. On the basis of these analyses, we predict that the trio of HRPKS, NRPKS, and ψACP-TE will make resorcylic acids that are structurally related to OA.

Heterologous Expression of Candidate Pathways Led to OA and SA Production. To examine the product profile of the ψACP-TE-containing pathways, we heterologously expressed Ma_OvaA, B, and C in the model fungus *Aspergillus nidulans* A1145 ΔSTΔEM strain.[24] This strain has been used in the reconstitution of fungal biosynthetic pathways and contains genetic deletions that abolished the biosynthesis of endogenous metabolites sterigmatocystin and emericellamide B.[24] Each of the three genes was cloned into separate episomal vectors and transformed into *A. nidulans*, and the resulting transformants were cultivated (see the Methods). Following 5 days of growth in CD-ST, the sample media were extracted and analyzed by liquid chromatography−mass spectrometry (LC-MS).

The coexpression of Ma_OvaA-C in *A. nidulans* produced four metabolites **1**−**4** (Figure 2B). The molecular weights (MWTs), as indicated by LC-MS for these compounds, are **1**: 252, **2**: 250, **3**: 224, and **4**: 222. The MWT, retention time, and

https://doi.org/10.1021/acssynbio.1c00309
ACS Synth. Biol. 2021, 10, 2159−2166

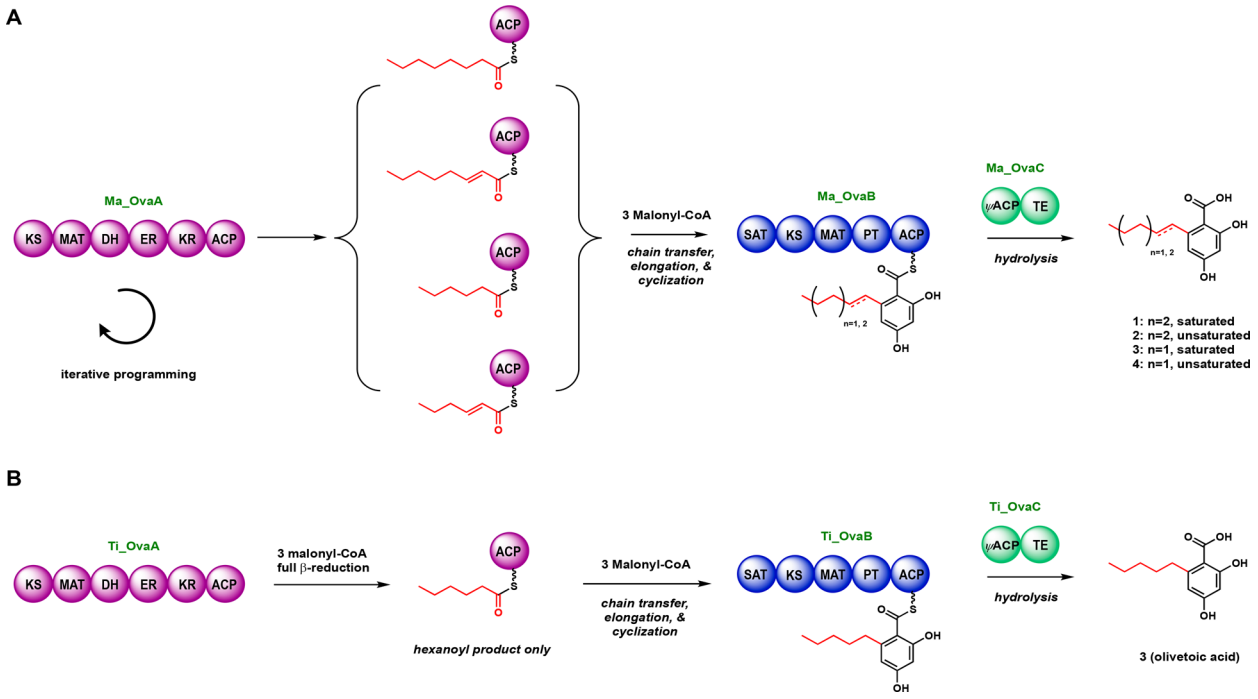

Figure 3. Proposed biosynthetic pathway of olivetolic acid and its analogues from *M. anisopliae* ARSEF23 and proposed olivetolic acid biosynthesis pathway of the homologous pair from *T. islandicus*. (A) HRPKS, Ma_OvaA, produces an ACP-bound starter unit that is promiscuous in alkyl chain length and saturation degree. NRPKS, Ma_OvaB, accepts any of the four starter units and further processes each into a resorcylyl-thioester. This is followed by hydrolysis of the thioester by Ma_OvaC to generate olivetolic acid **3** and its analogues (**1**, **2**, and **4**). (B) *T. islandicus* Ti_OvaA homologue produces only an ACP-bound hexanoyl that is accepted by the SAT domain of the Ti_OvaB to exclusively form olivetolic acid **3**.

UV absorption of **3** all matched those of OA. To obtain compounds for structural determination, we first optimized the culturing conditions to get high titers from the shake flask culture. By separately examining the organic extracts from cells and media, we determined that most of the compounds were secreted into the media. We also observed that a spore inoculum size of 10^4 spores/mL led to the highest titers of the four compounds, whereas inoculum sizes of 10^8 spores/mL and higher gave a low production of target compounds (Figure S4). Notably, when the molecules were produced at high titers, *A. nidulans* adopted a morphology of globular pellets. As the titer dropped upon increased inoculum size, *A. nidulans* grew as dispersed filaments (Figure S4). This is in agreement with previous reports that *Aspergillus niger* accumulated a high titer of citric acid when the fungus grew as globular pellets.[25]

From this simple optimization, these metabolites were purified from a large-scale culture and characterized by nuclear magnetic resonance (NMR) (Figures S11−S25 and Tables S3−S5). Compound **3** (80 mg/L) was confirmed to be OA, whereas **1** (∼1400 mg/L) was determined to be the C6-heptyl-substituted 2,4-dihydroxybenzoic acid, that is, SA (Figure 2, Table 1). Compound **2** (140 mg/L) showed a slightly red-shifted λ_{max} together with a decrease in the MWT of 2 mu compared with that of **1**, indicating that there is an extra degree of unsaturation that is conjugated to the aromatic ring. NMR analysis confirmed the presence of an olefin in the C6 alkyl substitution (Figure 2C). Whereas **4** was not isolated due to its lower titer (estimated to be 300 μg/L), on the basis of the UV absorption and the −2 mu decrease in the MWT compared with **3**, we propose the structure to be the olefin-containing version of **3** (Figure 2C). Significantly, the formation of **3** unveils a new microbial pathway to the cannabinoid precursor. The most abundantly produced SA (**1**) is a precursor to the octanoyl-primed, rare analog of cannabinoids, such as tetrahydrocannabiphorol (THCP). THCP represents the most potent natural CB1 and CB2 modulator isolated to date, with K_i values of 1.2 and 6.2 nM, respectively.[26] Hence the *M. anisopliae* pathway provides a facile route to access SA that can be further elaborated to the rare THCP and related molecules.

The biosynthesis of **1**−**4** confirms the hypothesis that a freestanding TE enzyme in a HRPKS/NRPKS-containing biosynthetic gene cluster is indicative of a resorcylic acid pathway. The biosynthesis of **1**−**4** requires all three enzymes, as we observed that omitting any of the three in *A. nidulans* completely abolished the biosynthesis of **1**−**4** (Figure S5). On the basis of the mechanism of dual PKS pathways, we assigned the functions of the enzymes, as shown in Figure 3A. HRPKS Ma_OvaA can produce a mixture of four different starter units, octanoyl-, 2-octenoyl-, hexanoyl-, and 2-hexenoyl-thioester, with octanoyl-thioester being the most abundant. The α,β-unsaturated starter units result from the enoylreductase (ER) domain of Ma_OvaA not functioning in the last iteration prior to the chain transfer to Ma_OvaB. The transfer of any of these four starter units to Ma_OvaB, facilitated by the SAT domain, is followed by three additional rounds of chain elongation and aldol cyclization by the product template (PT) domain to yield the resorcylyl-thioester attached to the ACP domain of Ma_OvaB. ψACP-TE Ma_OvaC then performs thioester hydrolysis to give **1**−**4**. The interaction between Ma_OvaB and Ma_OvaC may be enhanced by the ψACP domain, as previously described for the ψACP-MT system,[23] although this requires more detailed biochemical characterization.

Strategies toward Finding an Exclusive OA-Producing Pathway. Whereas the *M. anisopliae* cluster is able to make an abundant amount of SA, OA, the precursor to

https://doi.org/10.1021/acssynbio.1c00309
ACS Synth. Biol. 2021, 10, 2159−2166

common cannabinoids, is produced as a minor product. It is desirable to obtain a pathway that can exclusively produce OA for further optimization. Because removing HRPKS Ma_OvaA abolished the production of all related compounds, we reasoned that supplying a strain expressing Ma_OvaB and OvaC with a hexanoyl starter unit could lead to exclusive OA production. First, 1 mM *N*-acetylcysteamine thioester (SNAC) of hexanoate was supplied to a 25 mL *A. nidulans* culture on day 2 and cultured for 5 days to test if the KS domain of OvaB could directly capture it as the starter unit. However, when analyzing the sample on days 3, 4, and 5, no product could be detected from the culture, indicating that hexanoyl-SNAC was either not taken up by the cell or was not accepted (Figure S6). Next, we attempted to directly generate hexanoyl-CoA as a primer for Ma_OvaB by feeding 1 mM hexanoic acid and coexpressing the *Cannabis sativa* acyl-activating enzyme (CsAAE1) in combination with Ma_OvaB and Ma_OvaC. CsAAE1 was previously expressed in yeast to generate the hexanoyl-CoA for OAS incorporation.[8] We cultured the transformed strain in 25 mL of CD-ST medium in a 125 mL flask for 5 days following feeding with 1 mM hexanoic acid on day 2; however, no OA or related product was observed (Figure S6), suggesting that Ma_OvaB requires a hexanoyl starter unit attached to an upstream ACP, and small-molecule mimics are not compatible.

To pair Ma_OvaB with an HRPKS-like enzyme that can supply an ACP-bound hexanoyl starter unit, we turned to the related biosynthetic pathways of aflatoxin B1 and sterigmatocystin. Both utilize a pair of fatty-acid-synthase-like enzymes to synthesize a hexanoyl starter unit, which is then transferred by the SAT domain of the NRPKS for elongation and cyclization to yield the intermediate norsolorinic acid.[27,28] In the *A. nidulans* sterigmatocystin pathway, the StcK/StcJ enzymes have been paired with an NRPKS from the asperfuranone pathway to afford hexanoyl-primed hybrid products.[29] To test if crosstalk between StcJ/StcK and Ma_OvaB could take place, we coexpressed these enzymes with Ma_OvaC in the engineered *A. nidulans* ΔSTΔEM strain. Metabolic analysis showed that only OA was produced by this host at a titer of 5 mg/L. The lowered titer of OA using this combinatorial biosynthetic approach was likely due to nonnative and suboptimal protein−protein interactions between the ACP domain of StcJ/StcK and the SAT domain of Ma_OvaB. Nevertheless, this simple mix-and-match attempt showed that the product profile can indeed be manipulated by using different acyl donors.

Clusters homologous to the *M. anisopliae* cluster were discovered in *T. inflatum*, *M. rileyi*, and *T. islandicus* through bioinformatic analysis (Figure 2A). Although the clusters all share OvaA, B and C, their sequence identities are different (Figure S1), indicating the potential to generate resorcylic acids with different C6 substituents. Whereas OvaA, B, and C from *T. inflatum* (To_OvaABC) and *M. rileyi* (Mr_OvaABC) share high homology (∼84−89%) with the *M. anisopliae* cluster, those from *T. islandicus* (Ti_OvaABC) share low homology (∼46−52%). The heterologous expression of To_OvaABC in *A. nidulans* cultured in CD-ST revealed a similar product profile to Ma_OvaABC, albeit with a lower titer (750 mg/L for **1** and 40 mg/L for **3**) (Figure 2B, Table 1). Similarly, the heterologous expression of Mr_OvaABC showed that **1**−**4** can be detected from the *A. nidulans* extract at a lower titer (600 mg/L for **1** and 30 mg/L for **3**) (Table 1). Interestingly, when we heterologously expressed Ti_OvaABC genes from *T. islandicus*, **3** was exclusively produced at ∼60 mg/L, which is ∼12 times higher than that from the StcJ/StcK and Ma_OvaBC combination (Figure 2B, trace ii; Table 1). Therefore, we propose that Ti_OvaA, differentiated from Ma_OvaA, selectively produces an ACP-bound hexanoyl starter unit, which leads to the exclusive formation of **3** (Figure 3B). Ti_OvaABC therefore represents a new pathway to produce OA in microbial hosts.

Next, we explored the combinatorial mixing and matching of OvaA-C from *M. anisopliae* and *T. islandicus* to determine if an exclusive **3**-producing strain could be attained. We generated strains that coexpressed Ma_OvaA with Ti_OvaBC as well as Ti_OvaA with Ma_OvaBC. The heterologous expression of Ma_OvaA with Ti_OvaBC produced **1** and **3** at 75 and 4 mg/L, respectively (Table 1). This is almost 19 times lower than the heterologously expressing Ma_OvaABC. This result indicates that NRPKS does not have selectivity toward different C8 or C6 starter units. On the contrary, pairing of Ti_OvaA with Ma_OvaB-C led to the abolishment of **1**−**4** production, suggesting that the unnatural pair is not compatible.

There might be two factors contributing to the low titer (Ma_OvaA + Ti_OvaBC) and the abolishment of production (Ti_OvaA + Ma_OvaBC): (i) The most plausible cause is the disruption of specific protein−protein interactions between the domains participating in acyl chain transfer. (ii) Also, the rates of intermediate and final product formation by different clusters are different, in that each has been evolutionarily optimized to serve its respective biological host. The unnatural pairing can compromise the performance of the overall biosynthesis by a "rate-limiting" component such as Ti_OvaBC. Aside from the molecular recognition of the acyl chain by the SAT domain active site, a successful acyl chain transfer also requires complementary protein−protein interactions between the HRPKS ACP domain and the NRPKS SAT domain.[30,31] Previous studies have shown that although for some noncognate HRPKS-NRPKS pairs the acyl chain could occur and new products could emerge without any protein engineering efforts,[32] for others, the replacement of the SAT domain is necessary to compensate for the otherwise undermined interdomain communication.[29,33] Whereas the sequence identity between the ACPs of Ti_OvaA and Ma_OvaA is 62%, the identities between the NRPKS SAT domains of Ti_OvaB and Ma_OvaB are lowered to 48%. Such moderate sequence identity between the SAT domains implies that the recognition sites between ACP from noncognate HRPKS and SAT can be weakened or even abolished. Therefore, to generate a combination that exclusively produces **3** at a higher titer, protein engineering endeavors that improve the compatibility between unnatural HRPKS and NRPKS enzymes are necessary. Alternatively, further genome mining of related clusters may lead to one that can robustly produce OA in a heterologous host.

CONCLUSIONS

We have discovered a novel platform to produce OA and its analogues from filamentous fungi. The platform consists of an HRPKS and an NRPKS, known to produce resorcylic acid moieties in tandem, and a separate TE enzyme. This platform represents a new strategy to produce these cannabinoid precursors in microbes without relying on the OAS and OAC found in *Cannabis sativa*.

https://doi.org/10.1021/acssynbio.1c00309
ACS Synth. Biol. 2021, 10, 2159−2166

METHODS

Strain and Culture Conditions. *Metarhizium anisopliae* ARSEF23, *Tolypocladium inflatum*, *Metarhizium rileyi*, and *Talaromyces islandicus* were all separately grown on PDA (potato dextrose agar) for 3 days and then transferred to liquid PDB (PDA medium without agar) for the isolation of genomic DNA. *Aspergillus nidulans* 1145 was used as the model host for heterologous expression. *Aspergillus nidulans* 1145 was first grown on CD plates (10 g/L glucose, 20 g/L agar, 50 mL/L 20× nitrate salts, 1 mL/L trace elements) at 28 °C and then cultured in 25 mL of CD-ST medium (20 g/L starch, 20 g/L casamino acids, 50 mL/L 20× nitrate salts, and 1 mL/L trace elements) in a 125 mL flask at 28 °C and 250 rpm. 120 g of $NaNO_3$, 10.4 g of KCl, 10.4 g of $MgSO_4{\cdot}7H_2O$, and 30.4 g of KH_2PO_4 were dissolved in 1 L of distilled water to make 20× nitrate salts. 2.20 g of $ZnSO_4{\cdot}7H_2O$, 1.10 g of H_3BO_3, 0.50 g of $MnCl_2{\cdot}4H_2O$, 0.16 g of $FeSO_4{\cdot}7H_2O$, 0.16 g of $CoCl_2{\cdot}5H_2O$, 0.16 g of $CuSO_4{\cdot}5H_2O$, and 0.11 g of $(NH_4)_6Mo_7O_{24}{\cdot}4H_2O$ were dissolved in 100 mL of distilled water, with the pH being adjusted to 6.5 to make the trace element solution.

Plasmid Construction and Expression. Plasmids pYTU, pYTP, and pYTR containing auxotrophic markers for uracil (*pyrG*), pyridoxine (*pyroA*), and riboflavin (*riboB*), respectively, were digested and used as backbones to insert genes. The genes expressed (OvaA, OvaB, and OvaC) were amplified through polymerase chain reaction (PCR) using the genomic DNA of *Metarhizium anisopliae* ARSEF23, *Tolypocladium inflatum*, *Metarhizium rileyi*, and *Talaromyces islandicus* as templates. *StcJ/K* genes were amplified through PCR using the genomic DNA of *Aspergillus nidulans*. A *glaA* promoter and *trpC* terminator were amplified through PCR using pYTR as a template. The PCR fragments were transformed in yeast, and through homologous recombination, the plasmids pYTU-*glaA*-OvaB-*trpC*, pYTP-*glaA*-OvaC, and pYTR-*glaA*-OvaA-*trpC* were generated. Yeast transformation was performed using the Frozen-EZ Yeast Transformation II kit (Zymo Research). The plasmids were extracted from yeast and transformed into *E. coli* TOP10 by electroporation to isolate single plasmids. After extraction from *E. coli*, plasmid sequences were confirmed by sequencing. All three plasmids (pYTU-*glaA*-OvaB-*trpC*, pYTP-*glaA*-OvaC, pYTR-*glaA*-OvaA-*trpC*) were transformed into *A. nidulans* using standard protocols to form the OA-producing strain.[24] The strain was then cultured in 10 mL of CD-ST medium in a 50 mL Falcon tube and kept in a shaker at 28 °C and 250 rpm overnight. The next day, 25 μL of the culture was inoculated into 25 mL of CD-ST medium in a 125 mL flask and kept in a shaker at 28 °C and 250 rpm.

C. Sativa acyl-activating enzyme (CsAAE1) was ordered as a gene block from Integrated DNA Technologies (IDT). CsAAE1 was amplified through PCR and cloned onto the pYTR backbone containing the *gpdA* promoter. After following the previously outlined protocol to construct and confirm the sequence of plasmids, we transformed the pYTR-*gpda*-CsAAE1, pYTU-*glaA*-OvaB-*trpC*, and pYTP-*glaA*-OvaC plasmids into *A. nidulans*. After 5 days of growth at 37 °C on CD sorbitol plates, the strain was cultured in 25 mL of CD-ST medium in 125 mL flasks at 28 °C and 250 rpm. On day 2, 1 mM hexanoic acid was added to the culture, and analysis of the sample was done on days 3, 4, and 5.

***Aspergillus nidulans* Heterologous Expression.** To produce protoplasts, *Aspergillus nidulans* 1145 was grown on CD agar plates with 10 mM uridine, 5 mM uracil, 0.5 μg/mL of pyridoxine HCl, and 2.5 μg/mL of riboflavin at 37 °C for 4 days. *Aspergillus nidulans* 1145 spores were then inoculated in 25 mL of CD liquid medium containing 10 mM uridine, 5 mM uracil, 0.5 μg/mL of pyridoxine HCl and 2.5 μg/mL of riboflavin in a 250 mL flask and grown at 28 °C and 250 rpm for 16 h. The mycelia were harvested by centrifugation at 4300*g* for 20 min and washed with osmotic buffer (1.2 M $MgSO_4$, 10 mM sodium phosphate, pH 5.8). After harvesting by centrifugation once more, mycelia were then transferred to a 250 mL flask containing 10 mL of osmotic buffer with 30 mg of lysing enzymes from *Trichoderma* and 20 mg of yatalase. The mycelia were digested for 5 h at 28 °C and 80 rpm. The cells were then transferred to a 50 mL centrifuge tube, overlaid gently by 10 mL of trapping buffer (0.6 M sorbitol, 0.1 M Tris-HCI, pH 7.0), and centrifuged at 5300 rpm for 20 min at 4 °C. Two layers appeared with the protoplasts at the interface of the two layers. The protoplasts were collected and placed in a sterile 15 mL Falcon tube, washed with 10 mL of STC buffer (1.2 M sorbitol, 10 mM $CaCl_2$, 10 mM Tris-HCI, pH 7.5), and centrifuged for 10 min at 4300*g* and 4 °C. The protoplasts were then suspended in 1 mL of STC buffer, aliquoted in 60 μL increments in 1.5 mL microcentrifuge tubes, and stored at −80 °C.

For the transformation, 2 μL of each plasmid needed for the heterologous expression was added to the 60 μL aliquots of *Aspergillus nidulans* 1145 protoplasts and then kept on ice for 60 min. The aliquots were then mixed with 600 μL of PEG solution (60% PEG, 50 mM calcium chloride, and 50 mM Tris-HCl, pH 7.5), incubated at room temperature for 20 min, and plated on CD sorbitol agar plates (CD solid medium with 1.2 M sorbitol and the appropriate supplements, according to the markers on the plasmids). Plates were then incubated at 37 °C for 3−5 days.

For hexanoyl-SNAC feeding, the *A. nidulans* strain containing pYTU-*glaA*-OvaB-*trpC* and pYTP-*glaA*-OvaC plasmids was cultured in 25 mL of CD-ST in a 125 mL flask at 28 °C and 250 rpm for 5 days. On day 2, 1 mM hexanoyl-SNAC was fed into the cultures, and analysis of the sample was done on days 3, 4, and 5.

Sample Preparation, Detection, Isolation, and Quantification. Individual colonies from transformation plates were cultured in 25 mL of liquid CD-ST medium in 125 mL flasks and grown for 5 days. On the sixth day, 500 μL of cells and medium was extracted with 800 μL of an ethyl acetate acid mix (1:9 methanol to ethyl acetate with 0.1% formic acid). The extracted sample was then dried and placed in 50 μL of methanol and then loaded onto the LC-MS.

LC-MS analyses were performed using a Shimadzu 2020 LC-MS (Phenomenex Kinetex, 1.7 μm, 2.0 × 100 mm, C-18 column) using positive- and negative-mode electrospray ionization. The elution method was a linear gradient of 5−95% (v/v) acetonitrile/water in 13.25 min followed by 95% (v/v) acetonitrile/water for 4.75 min with a flow rate of 0.3 mL/min. The LC mobile phases were supplemented with 0.1% formic acid (v/v).

The large-scale production of compounds for the purpose of isolation and structural determination was carried out by cultivating transformants in 1 L of CD-ST. After 5 days of growth at 28 °C, the media were extensively extracted with acidified ethyl acetate. The extract was concentrated under reduced pressure. Purification was carried out as previously reported with slight modifications.[23] In brief, the residue was loaded to a RediSep Rf Gold reversed-phase C18 column on a

https://doi.org/10.1021/acssynbio.1c00309
ACS Synth. Biol. 2021, 10, 2159−2166

Teledyne Combi-Flash system. Subsequently, high-performance liquid chromatography (HPLC) purifications were performed with a Phenomenex Kinetex column (5 μ, 10.0 × 250 mm, C18) using a Shimadzu ultrafast liquid chromatography (UFLC) system. For the HPLC purification, a flow rate of 4 mL/min with solvents A (0.1% formic acid in water) and B (0.1% formic acid in acetonitrile) was used. NMR spectra of **1**−**3** were acquired on a Bruker AV500 spectrometer with a 5 mm dual cryoprobe (^{1}H 500 MHz, ^{13}C 125 MHz).

Quantification of the compounds was done by first making a standard curve on the HPLC. Known concentrations of isolated compound were analyzed on the HPLC, and a standard curve was constructed correlating the area under the UV peak corresponding to the compound to the concentration of the compound. Cultured samples were then extracted and analyzed on the HPLC, where the area under the UV peak was used to calculate the concentration of the sample.

■ ASSOCIATED CONTENT

Supporting Information

The Supporting Information is available free of charge at https://pubs.acs.org/doi/10.1021/acssynbio.1c00309.

Experimental details, standard curves, homologous clusters, chromatograms, and spectroscopic data (PDF)

■ AUTHOR INFORMATION

Corresponding Author

Yi Tang − *Department of Chemical and Biomolecular Engineering, Chemistry and Biochemistry, and California NanoSystems Institute (CNSI), University of California Los Angeles, Los Angeles, California 90095, United States;* orcid.org/0000-0003-1597-0141; Email: yitang@ucla.edu

Authors

Ikechukwu C. Okorafor − *Department of Chemical and Biomolecular Engineering, University of California Los Angeles, Los Angeles, California 90095, United States*

Mengbin Chen − *Department of Chemical and Biomolecular Engineering, University of California Los Angeles, Los Angeles, California 90095, United States;* orcid.org/0000-0001-6135-8661

Complete contact information is available at: https://pubs.acs.org/10.1021/acssynbio.1c00309

Author Contributions

‖I.C.O. and M.C. contributed equally.

Notes

The authors declare the following competing financial interest(s): The contents of this paper are the subject of a patent application submitted by UCLA. Yi Tang is a founder of Hexagon Biosciences.

■ ACKNOWLEDGMENTS

This work was supported by grant R35GM118056 from the NIH to Y.T. and by the California NanoSystems Institute and the Noble Family Innovation Fund. I.C.O. is a BioPacific summer fellow supported by a National Science Foundation (NSF) cooperative agreement (DMR-1933487). Structural characterization by NMR was supported by the NSF under equipment grant no. CHE-1048804. We thank Drs. John Billingsley and Yang Hai for insightful discussions and Abbegayle Young for assistance with the bioinformatic analysis.

■ REFERENCES

(1) Shah, S. A.; Gupta, A. S.; Kumar, P. Emerging role of cannabinoids and synthetic cannabinoid receptor 1/cannabinoid receptor 2 receptor agonists in cancer treatment and chemotherapy-associated cancer management. *J. Cancer Res. Ther.* **2021**, *17*, 1−9.

(2) Stott, C. G.; Guy, G. W. Cannabinoids for the Pharmaceutical Industry. *Euphytica* **2004**, *140*, 83−93.

(3) Jetly, R.; Heber, A.; Fraser, G.; Boisvert, D. The efficacy of nabilone, a synthetic cannabinoid, in the treatment of PTSD-associated nightmares: A preliminary randomized, double-blind, placebo-controlled cross-over design study. *Psychoneuroendocrinology* **2015**, *51*, 585−588.

(4) Beal, J. E.; Olson, R.; Laubenstein, L.; Morales, J. O.; Bellman, P.; Yangco, B.; Lefkowitz, L.; Plasse, T. F.; Shepard, K. V. Dronabinol as a treatment for anorexia associated with weight loss in patients with AIDS. *J. Pain Symptom Manage.* **1995**, *10*, 89−97.

(5) National Academies of Sciences, Engineering, and Medicine. The Health Effects of Cannabis and Cannabinoids: The Current State of Evidence and Recommendations for Research. *Nat. Acad. Press* **2017**, 377−390.

(6) Gagne, S. J.; Stout, J. M.; Liu, E.; Boubakir, Z.; Clark, S. M.; Page, J. E. Identification of olivetolic acid cyclase from *Cannabis sativa* reveals a unique catalytic route to plant polyketides. *Proc. Natl. Acad. Sci. U. S. A.* **2012**, *109*, 12811−12816.

(7) Tan, Z.; Clomburg, J. M.; Gonzalez, R. Synthetic Pathway for the Production of Olivetolic Acid in *Escherichia coli*. *ACS Synth. Biol.* **2018**, *7*, 1886−1896.

(8) Luo, X.; Reiter, M. A.; d'Espaux, L.; Wong, J.; Denby, C. M.; Lechner, A.; Zhang, Y.; Grzybowski, A. T.; Harth, S.; Lin, W.; Lee, H.; Yu, C.; Shin, J.; Deng, K.; Benites, V. T.; Wang, G.; Baidoo, E. E. K.; Chen, Y.; Dev, I.; Petzold, C. J.; Keasling, J. Complete biosynthesis of cannabinoids and their unnatural analogues in yeast. *Nature* **2019**, *567*, 123−126.

(9) Ismed, F.; Farhan, A.; Bakhtiar, A.; Zaini, E.; Nugraha, Y. P.; Dwichandra Putra, O.; Uekusa, H. Crystal structure of olivetolic acid: a natural product from *Cetrelia sanguinea* (Schaer.). *Acta Crystallogr. E. Crystallogr. Commun.* **2016**, *72*, 1587−1589.

(10) Blatt-Janmaat, K.; Qu, Y. The Biochemistry of Phytocannabinoids and Metabolic Engineering of Their Production in Heterologous Systems. *Int. J. Mol. Sci.* **2021**, *22*, 2454.

(11) Zhou, H.; Zhan, J.; Watanabe, K.; Xie, X.; Tang, Y. A polyketide macrolactone synthase from the filamentous fungus *Gibberella zeae*. *Proc. Natl. Acad. Sci. U. S. A.* **2008**, *105*, 6249−54.

(12) Chen, H.; Du, L. Iterative polyketide biosynthesis by modular polyketide synthases in bacteria. *Appl. Microbiol. Biotechnol.* **2016**, *100*, 541−557.

(13) Zhou, H.; Qiao, K.; Gao, Z.; Vederas, J. C.; Tang, Y. Insights into Radicicol Biosynthesis via Heterologous Synthesis of Intermediates and Analogs. *J. Biol. Chem.* **2010**, *285*, 41412−41421.

(14) Zhou, H.; Qiao, K.; Gao, Z.; Meehan, M. J.; Li, J. W. H.; Zhao, X.; Dorrestein, P. C.; Vederas, J. C.; Tang, Y. Enzymatic Synthesis of Resorcylic Acid Lactones by Cooperation of Fungal Iterative Polyketide Synthases Involved in Hypothemycin Biosynthesis. *J. Am. Chem. Soc.* **2010**, *132*, 4530−4531.

(15) Reeves, C. D.; Hu, Z.; Reid, R.; Kealey, J. T. Genes for the biosynthesis of the fungal polyketides hypothemycin from *Hypomyces subiculosus* and radicicol from *Pochonia chlamydosporia*. *Appl. Environ. Microbiol.* **2008**, *74*, 5121−5129.

(16) Wang, M.; Zhou, H.; Wirz, M.; Tang, Y.; Boddy, C. N. A Thioesterase from an Iterative Fungal Polyketide Synthase Shows Macrocyclization and Cross Coupling Activity and May Play a Role in Controlling Iterative Cycling through Product Offloading. *Biochemistry* **2009**, *48*, 6288−6290.

(17) Heberlig, G. W.; Wirz, M.; Wang, M.; Boddy, C. N. Resorcylic Acid Lactone Biosynthesis Relies on a Stereotolerant Macrocyclizing Thioesterase. *Org. Lett.* **2014**, *16*, 5858−5861.

(18) Xu, W.; Chooi, Y. H.; Choi, J. W.; Li, S.; Vederas, J. C.; Da Silva, N. A.; Tang, Y. LovG: the thioesterase required for dihydromonacolin L release and lovastatin nonaketide synthase turnover in lovastatin biosynthesis. *Angew. Chem., Int. Ed.* **2013**, *52*, 6472−6475.
(19) Weber, T.; Blin, K.; Duddela, S.; Krug, D.; Kim, H. U.; Bruccoleri, R.; Lee, S. Y.; Fischbach, M. A.; Müller, R.; Wohlleben, W.; Breitling, R.; Takano, E.; Medema, M. H. antiSMASH 3.0-a comprehensive resource for the genome mining of biosynthetic gene clusters. *Nucleic Acids Res.* **2015**, *43*, W237−243.
(20) Keating, D. H.; Carey, M. R.; Cronan Jr, J. E. The unmodified (apo) form of *Escherichia coli* acyl carrier protein is a potent inhibitor of cell growth. *J. Biol. Chem.* **1995**, *270*, 22229−22235.
(21) Flugel, R. S.; Hwangbo, Y.; Lambalot, R. H.; Cronan, J. E.; Walsh, C. T. Holo-(acyl carrier protein) synthase and phosphopantetheinyl transfer in *Escherichia coli*. *J. Biol. Chem.* **2000**, *275*, 959−968.
(22) Crawford, J. M.; Vagstad, A. L.; Ehrlich, K. C.; Udwary, D. W.; Townsend, C. A. Acyl-carrier protein-phosphopantetheinyltransferase partnerships in fungal fatty acid synthases. *ChemBioChem* **2008**, *9*, 1559−1563.
(23) Chen, M.; Liu, Q.; Gao, S. S.; Young, A. E.; Jacobsen, S. E.; Tang, Y. Genome mining and biosynthesis of a polyketide from a biofertilizer fungus that can facilitate reductive iron assimilation in plant. *Proc. Natl. Acad. Sci. U. S. A.* **2019**, *116*, 5499−5504.
(24) Liu, N.; Hung, Y. S.; Gao, S. S.; Hang, L.; Zou, Y.; Chooi, Y. H.; Tang, Y. Identification and Heterologous Production of a Benzoyl-Primed Tricarboxylic Acid Polyketide Intermediate from the Zaragozic Acid A Biosynthetic Pathway. *Org. Lett.* **2017**, *19*, 3560−3563.
(25) Papagianni, M. Advances in citric acid fermentation by Aspergillus niger: Biochemical aspects, membrane transport and modeling. *Biotechnol. Adv.* **2007**, *25*, 244−263.
(26) Citti, C.; Linciano, P.; Russo, F.; Luongo, L.; Iannotta, M.; Maione, S.; Laganà, A.; Capriotti, A. L.; Forni, F.; Vandelli, M. A.; Gigli, G.; Cannazza, G. A novel phytocannabinoid isolated from *Cannabis sativa* L. with an *in vivo* cannabimimetic activity higher than Δ^9-tetrahydrocannabinol: Δ^9-Tetrahydrocannabiphorol. *Sci. Rep.* **2019**, *9*, 20355.
(27) Hitchman, T. S.; Schmidt, E. W.; Trail, F.; Rarick, M. D.; Linz, J. E.; Townsend, C. A. Hexanoate Synthase, a Specialized Type I Fatty Acid Synthase in Aflatoxin B_1 Biosynthesis. *Bioorg. Chem.* **2001**, *29*, 293−307.
(28) Brown, B. W.; Yu, J. H.; Kelkar, H. S.; Fernandes, M.; Nesbitt, T. C.; Keller, N. P.; Adams, T. H.; Leonard, T. J. Twenty-five coregulated transcripts define a sterigmatocystin gene cluster in *Aspergillus nidulans*. *Proc. Natl. Acad. Sci. U. S. A.* **1996**, *93*, 1418−1422.
(29) Liu, T.; Chiang, Y. M.; Somoza, A. D.; Oakley, B. R.; Wang, C. C. C. Engineering of an "Unnatural" Natural Product by Swapping Polyketide Synthase Domains in *Aspergillus nidulans*. *J. Am. Chem. Soc.* **2011**, *133*, 13314−13316.
(30) Zhang, W.; Tang, Y. Combinatorial Biosynthesis of Natural Products. *J. Med. Chem.* **2008**, *51*, 2629−2633.
(31) Crawford, J. M.; Dancy, B. C. R.; Hill, E. A.; Udwary, D. W.; Townsend, C. A. Identification of a starter unit acyl-carrier protein transacylase domain in an iterative type I polyketide synthase. *Proc. Natl. Acad. Sci. U. S. A.* **2006**, *103*, 16728−16733.
(32) Xu, Y.; Zhou, T.; Zhang, S.; Espinosa-Artiles, P.; Wang, L.; Zhang, W.; Lin, M.; Gunatilaka, A. A. L.; Zhan, J.; Molnár, I. Diversity-oriented combinatorial biosynthesis of benzenediol lactone scaffolds by subunit shuffling of fungal polyketide synthases. *Proc. Natl. Acad. Sci. U. S. A.* **2014**, *111*, 12354−12359.
(33) Bai, J.; Lu, Y.; Xu, Y. M.; Zhang, W.; Chen, M.; Lin, M.; Gunatilaka, A. A. L.; Xu, Y.; Molnár, I. Diversity-Oriented Combinatorial Biosynthesis of Hybrid Polyketide Scaffolds from Azaphilone and Benzenediol Lactone Biosynthons. *Org. Lett.* **2016**, *18*, 1262−1265.

https://doi.org/10.1021/acssynbio.1c00309
ACS Synth. Biol. 2021, 10, 2159−2166